Journal of The
Electrochemical Society

The Electrochemical Society
Advancing solid state & electrochemical science & technology

Investigation of Electrochemical Oxidation Mechanism, Thermodynamic Parameters and Sensor Design for Analgesic and Relaxant Drug: Phenyramidol in Aqueous Medium by NH_2-MWCNT

To cite this article: Hamideh Imanzadeh *et al* 2019 *J. Electrochem. Soc.* **166** B1209

View the article online for updates and enhancements.

You may also like

- Electrochemical Sensing of Phenylbutazone using Multi-Walled Carbon Nanotube Paste Electrode in Pharmaceutical and Biological Fluids
Yuvarajgouda Patil, Manjunath Megalamani, Jyothi Abbar et al.
- Polyethylenimine-Multi-Walled Carbon Nanotubes/Glassy Carbon Electrode as an Efficient Sensing Platform for Promethazine
Raissa C. de Oliveira, Camila P. Sousa, Simone Morais et al.
- Analytical Eco-Scale for Evaluating the Greenness of Advanced Voltammetric Method Used for the Simultaneous Analysis of Combined Urinary Tract Infection Drugs in Different Matrices
Ola G. Hussein, Eman S. Elzanfaly, Hala E. Zaazaa et al.

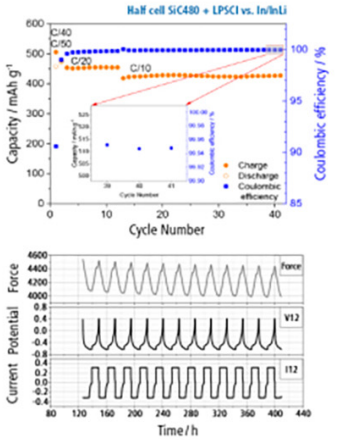
The New PAT-Cell-Solid!

EL-CELL®
electrochemical test equipment

Cycle Solid-State Batteries Under Controlled Pressure of up to 300 MPa (6 mm Diameter)!



- Adjust and measure a force of up to 9000 N on the cell stack!
  Force adjustment possible throughout the entire experiment
- Built-in force, and temperature sensors!
  With optional gas pressure sensor and gas in- and outlet
- PAT-Solid-Core for easy assembly and reproducible results!
  Press and cycle solid-state batteries with 6 or 10 mm electrode diameter
- Cableless and highly sealed battery test cell!
  For precise long-term measurements of solid-state cell chemistries



Learn more on our product website:
Scan me!

Download the data sheet (PDF):
Scan me!

Or contact us directly:
+49 40 79012-734
sales@el-cell.com
www.el-cell.com

This content was downloaded from IP address 161.9.196.133 on 25/09/2026 at 03:26

Journal of The Electrochemical Society, **166** (13) B1209-B1216 (2019)
0013-4651/2019/166(13)/B1209/8/$38.00 © The Electrochemical Society
All rights, including for text and data mining, AI training, and similar technologies, are reserved.

Investigation of Electrochemical Oxidation Mechanism, Thermodynamic Parameters and Sensor Design for Analgesic and Relaxant Drug: Phenyramidol in Aqueous Medium by NH_2*f*MWCNT

Hamideh Imanzadeh,[1,2] Nurgul K. Bakirhan,[3,z] Biuck Habibi,[2] and Sibel A Ozkan[1,z]

[1]*Ankara University, Faculty of Pharmacy, Department of Analytical Chemistry, 06560 Ankara, Turkey*
[2]*Electroanalytical Chemistry Laboratory, Department of Chemistry, Faculty of Sciences, Azarbaijan Shahid Madani University, Tabriz, Iran*
[3]*University of Health Sciences, Gulhane Faculty of Pharmacy, Department of Analytical Chemistry, Ankara, Turkey*

In this study, the electrochemical oxidation mechanism of phenyramidol HCl (PhA) was investigated in aqueous medium. An amine functionalized multi walled carbon nanotube (NH_2*f*MWCNT) modified glassy carbon electrode (GCE) was used as a sensitive and fast sensor for the determination of PhA. Scanning electron microscopy (SEM) with Energy Dispersive X-Ray (EDX), analysis and electrochemical impedance spectroscopy (EIS) were applied for investigation of surface morphology. Cyclic voltammetry (CV) differential pulse voltammetry (DPV) and adsorptive stripping differential pulse voltammetry (AdSDPV) methods were employed to compare the redox responses of PhA on the surface of bare and modified electrode with NH_2*f*MWCNTs. The results showed a considerable enhancement in the peak current of PhA with AdSDPV. A linear calibration curve was obtained in the concentration ranges of 0.8–100 μM, with a detection limit of 6.13×10^{-8} M and 2.78×10^{-8} M from peaks 1 and 2, respectively. The proposed procedure was easily and sensitively applied for the determination of PhA in human serum samples and tablet dosage form with satisfactory recovery value (recovery >99%).
© 2019 The Electrochemical Society. [DOI: 10.1149/2.0971913jes]

Manuscript submitted June 7, 2019; revised manuscript received August 18, 2019. Published September 3, 2019.

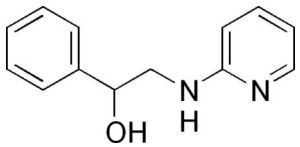
The phenyramidol HCl (PhA) (Scheme 1) was introduced in the 19th century for the first time in clinical trials.[1] PhA is a powerful (non-narcotic) painkiller and moderately effective, which acts as a muscle relaxant.[2] Generally, this drug is used in patients with chronic muscular disorders and it is existed as tablet (400 mg) or ampule (800 mg/3 mL).[3] Phenyramidol analysis was performed using liquid chromatography and mass detection.[4]

So far, the determination of PhA has not been reported with voltammetric methods. In this work, for the first time we have investigated PhA redox behavior with voltammetric method and its fully validated analysis. Recent progress of nanomaterials, especially carbon nanostructures have created new perspectives owing to their unique physical and chemical attributes, on design of modified electrodes in electrochemical sensors.[5–8] Among carbon nanomaterials, carbon nanotubes (CNTs) are mostly used materials.[9] The carbon nanotubes were discovered in 1991 and released to the world.[10] The carbon nanotubes are obtained from the complexity of graphite sheets with a structure similar to the honey shoulder. If the carbon nanotube only contains a tube of graphite, it is called as single-walled nanotube and, if it contains a number of concentric tubes, is called a multi-walled nanotubes.[11,12] They have several advantages as an electrochemical sensors, including wide potential window, great surface area, fast electron transfer rate and high electrical conductivity.[13] In order to improve solubility[11,14–17] and absorption capacity,[12] CNTs is functionalized with groups such as: carboxyl, hydroxyl, amino and thiol groups. In recent years, *f*MWCNT has been applied as modifier for the determination of pharmaceutical sensors such as detection of clopidogrel bisulfate,[18] entacapone,[19] bisphenol F,[20] troponin T[21] pazufloxacin[22] hydroquinone[23] and melamine[24] with high sensitivity and repeatability.

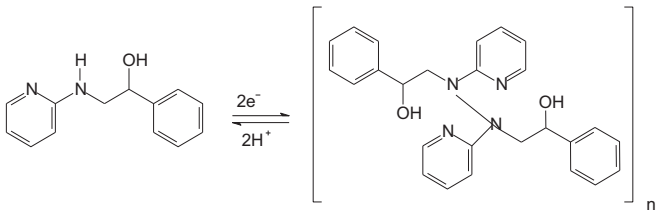
Research and development of clinical and pharmaceutical industry need sensitive, rapid and accurate assay of drugs from biological samples and their dosage forms. At this point, sensor techniques have great interest over recent years. Heretofore, no report is accessible on the measurement of PhA. Our aim is develop of an electrochemical sensor for the sensitive determination PhA with modified sensor. The oxidation mechanism was investigated with in detailed electrochemical studies. Up to this date, there is no any suggestion with redox mechanism of PhA in aqueous solutions. Voltammetric technique was also optimized with its parameters to obtained well-defined oxidation response of PhA. The results of this research showed that the simple, fast and sensitive assay method and sensor have been developed. Modified electrode can be used in commercial forms and biological samples for detection of PhA.

Experimental

Reagents and chemicals.—NH_2 functionalized multi-walled carbon nanotubes (NH_2 *f*MWCNTs) was obtained from DropSens (Llanera, Spain). They have a specific surface BET of 300 m^2/g, an average diameter of 10 nm and an average length of 1.5 μm. The standard reference compound, PhA was purchased from RECORDATI Pharmacy, Turkey. Human serum from human male AB plasma was purchased from Sigma–Aldrich (St. Louis, MO, no need for ethical committee permission) and stored at −20°C. A stock solution of 1.0×10^{-3} M PhA was prepared in water. Different buffer solutions such as phosphate (pH 2.0, 3.0, 6.0, 7.0, 8.0) and acetate pH 3.5, 4.5, 5.5 were used for electrochemical measurements. All buffer solutions were prepared with bi-distilled water (18.2 MΩ cm). $Na_2HPO_4$and $NaH_2PO_4{\cdot}2H_2O$ were obtained from Riedel-de Haen. H_3PO_4, acetic acid were purchased from Sigma–Aldrich. All other chemicals such as H_2SO_4, NaCl, $NaNO_3$, ascorbic acid, uric acid, potassium ferrocyanide,



Scheme 1. Chemical structure of PhA.



Scheme 2. Possible oxidation mechanism of PhA on NH_2fMWCNT/GCE.

[z]E-mail: ozkan@pharmacy.ankara.edu.tr; nurgulk44@gmail.com

N,N-dimethylformamide (DMF) were purchased at analytical reagent grade from Merck.

Apparatus.—AUTOLAB-PGSTAT 302 (Eco Chemie, Utrecht, The Netherlands) was used as electrochemical instrument for performing voltammetric experiments. All electrochemical experiments were applied in a three-electrode system cell (Ag/AgCl (BAS; 3 M KCl) as a reference electrode, Pt wire (BASi) as the counter electrode, bare glassy carbon electrode (3 mm diameter GCE) and NH_2*f*MWCNT/GCE as the working electrode. A pH meter (Model 538, WTW, Austria) (reference electrode-glass electrode) with an uncertainty of 0.05 was applied for the preparing of the buffer solutions. Scanning electron microscopy (SEM) and energy dispersive X-ray (EDX) analysis using ZEISS EVO 40 (Merlin, Carl Zeiss) were used to characterize of the modified electrode (NH_2*f*MWCNTs/GCE).

Preparation of the modified GCE.—MWCNT, COOH*f*MWCNT, NH_2*f*MWCNT, reduced graphene oxide (RGO) nanoparticles were weighed as 1 mg and prepared in 1 mL dimethylformamide solution and sonicated for 2 hours. ZnO, TiO_2 suspensions were prepared in 1 mL deionized water and sonicated for 10 min.

Glassy carbon electrodes (GCE) were polished by the alumina powder (0.05 μm) on a polishing pad and rinsed with distilled water. Then, 10 μL of the each prepared suspensions were separately dropped on the GCE and allowed to dry in a vacuum oven during 10 min. The dried modified GCEs were activated with CV between 0 and 1.7 V (0.1 V/s scan rate) with 3 cycles in buffer solution then used for the detection of PhA.

Analytical procedure.—DPV was applied between 0 and 1.7 V (Scan rate: 20 mV/s; Step potential: 5 mV; Amplitude: 20 mV) in the presence of 0.1 mM PhA at phosphate buffer of pH 3.0. The scan rate study presented an adsorption controlled process occurring on the electrode surface. Therefore, the further experiments were realized with AdSDPV. The quantitative detection was applied with AdSDPV with its optimum accumulation time and accumulation potential conditions as 30 s and −0.2 V between 0 and 1.7 V range.

Preparation of serum sample.—In order to analyze PhA in synthetic serum sample, 1.0 mL of 1.0×10^{-2} M standard PhA was mixed with 3.6 mL serum sample and 5.4 mL of acetonitrile. The mixture was centrifuged for 10 min at 3500 rpm to separate the protein residues and then the supernatant was taken carefully. This human serum stock was diluted with pH 3.0 phosphate buffer (PB) solution for calibration curve and recovery experiments.

Results and Discussion

Characterization of the NH_2fMWCNTs /GCE.—*Investigation of morphology on NH_2f*MWCNTs /GCE.*—To study the surface morphology of the NH_2f*MWCNTs modified glassy carbon electrode, SEM armed with EDX analysis has been employed. Figs. 1A and 1C depict the SEM graphs of unmodified GCE and NH_2*f*MWCNTs film on the surface of the GCE, respectively. Figs. 1B and 1C presented deposition of NH_2*f*MWCNTs suspension on the surface of bare GCE. NH_2*f*MWCNTs showed a uniform and rough surface on GCE. If scale was increased, nano forms were clearly observed (Fig. 1C). EDX spectrum of NH_2*f*MWCNTs film in Fig. 1D confirmed the attendance of oxygen and carbon on modified electrode. These atoms were found with lower percentage on bare GCE.

Electrochemical impedance spectroscopy (EIS).—Fig. 2A shows the cyclic voltammograms of 5 mM $Fe(CN)_6^{3-/4-}$ at GCE and NH_2*f*MWCNTs/GCE. The peak current value increased in the presence of nanotubes on GCE. NH_2*f*MWCNT enhanced easy electron transferred process on GCE.

EIS was used to check the changes in the charge transfer resistance (Rct) of modified and bare GCE (Fig. 2B) between 0.1 and 10^5 Hz in 5 mM potassium ferrocyanide solution. Inset of Fig. 2B is the equivalent circuit used for fitting the data, where R_e stands for resistance of electrolytic solution and CPE for constant phase element. In general, the Nyquist plot of the impedance spectrum have two parts: a semicircle portion at higher frequencies that related to the process of kinetic restriction of the electrochemical reaction (Rct), and a linear section at lower frequencies related to diffusion process) Warburg resistance: RW. (Fig. 2B showed that modified electrode (Rct = 147 Ω) had smaller diameter of semicircle than bare GCE (Rct = 3.5 kΩ) It means that faster electron transfer occurs at the surface of NH_2*f*MWCNTs/GCE than bare GCE due to high surface to volume ratio and consequent availability of more active sites for the redox probe. NH_2*f*MWCNT nanoparticles may increase conductivity on the surface and decrease charge transferred resistance. It is generally known that the wall of MWCNTs is built up by the π electron delocalization from sp2 hybrid orbitals, and the presence of functional groups such as the amino group increase the density of the electrons and strengthen the electron delocalization of MWNTs and reduce the resistance.[25–27]

The slope acquired from a linear plot of I_{pa} versus $\nu^{1/2}$ was utilized to estimate the active surface area of both bare unmodified and modified electrodes according to the Randles Sevcik equation (Eq. 1).

$$I_p = 2.69 \times 10^5 n^{2/3} A D^{1/2} V^{1/2} C \quad [1]$$

In this equation D, diffusion coefficient is 7.6×10^{-6} $cm^2 s^{-1}$[28], n denotes the number of electron transferred, C_0 is the concentration of $K_3Fe[CN]_6$ and $K_4Fe[CN]_6$ in solution, I_P is the peak current (μA), A represents active surface area (cm^2) of the electrode. The effective surface area of the bare GCE and NH_2*f*MWCNTs/GCE were estimated to be 0.034 and 0.093 cm^2, respectively. These results show an increase in surface area after modification, which means NH_2*f*MWCNT/GCE supplys higher surface area to catalyze the respective reaction on its surface.

Electrochemical behavior of PhA.—The cyclic voltammograms (CVs) for both electrodes: bare GCE (purple line) and NH_2*f*MWCNTs/GCE (red line) in the presence of 0.1 mM PhA at phosphate buffer of pH 3.0 were recorded in the potential range 0.0 and 1.7 V versus Ag/AgCl (Fig. 3A). The electrochemical response of PhA demonstrated an irreversible behavior with peaks two weak oxidation around 1.023 V and 1.229 V with anodic peak current of $I_{P1} = 2.760$ μA and $I_{P2} = 6.080$ μA for unmodified GCE in scan rate of 100 mV s^{-1}. As shown in Fig. 3A. at NH_2-*f*MWCNT modified electrode the oxidation peaks currents of PhA are significantly increased. The enhancement in peak currents with peak potential shift to less positive potentials at NH_2*f*MWCN/GCE displays efficient electrocatalysis toward oxidation of PhA.[29–31] A notable increase of the peak currents for this is owing to the presence of carbon nanotubes at the electrode surface that has caused a striking increase in the conductive surface and molecules of PhA can penetrate through the conductive porous channels onto the modified electrode more simply, leading to higher selectivity and sensitivity. In addition, layers of MWCNTs could form π-π bonds with PhA molecules, therefore the electron transfer of PhA at the surface of the modified electrode is facilitated and enhances the electrocatalytic effect of PhA to attain $I_{P1} = 12.01$ μA and $I_{P2} = 10.44$ μA .

Since the oxidation of PhA was considered, therefore oxidation peaks were used for further investigation. Fig. 3B shows the differential pulse voltammograms (DPV) of unmodified (red line) and modified electrode (purple line) for 0.1 mM PhA. Unmodified electrode indicates the three peaks with low current intensity for PhA, which indicates poor sensitivity. It can be clearly seen at Fig. 3B that there is a significant increase in the first and second peak signals, as well as the potential shift to the lower potentials for both peaks (first peak: 0.997 V, second peak: 1.198 V), which suggesting catalytic activity of nanotubes toward electrooxidation of PhA.

Different modifiers were used for sensitive PhA response as well as NH_2MWCNT such as MWCNT, carboxylic acid functionalized MWCNT (COOH*f*MWCNT), carbon quantum dot (CQD), zinc oxide (ZnO), titanium oxide (TiO_2) and reduced graphene oxide (RGO). The

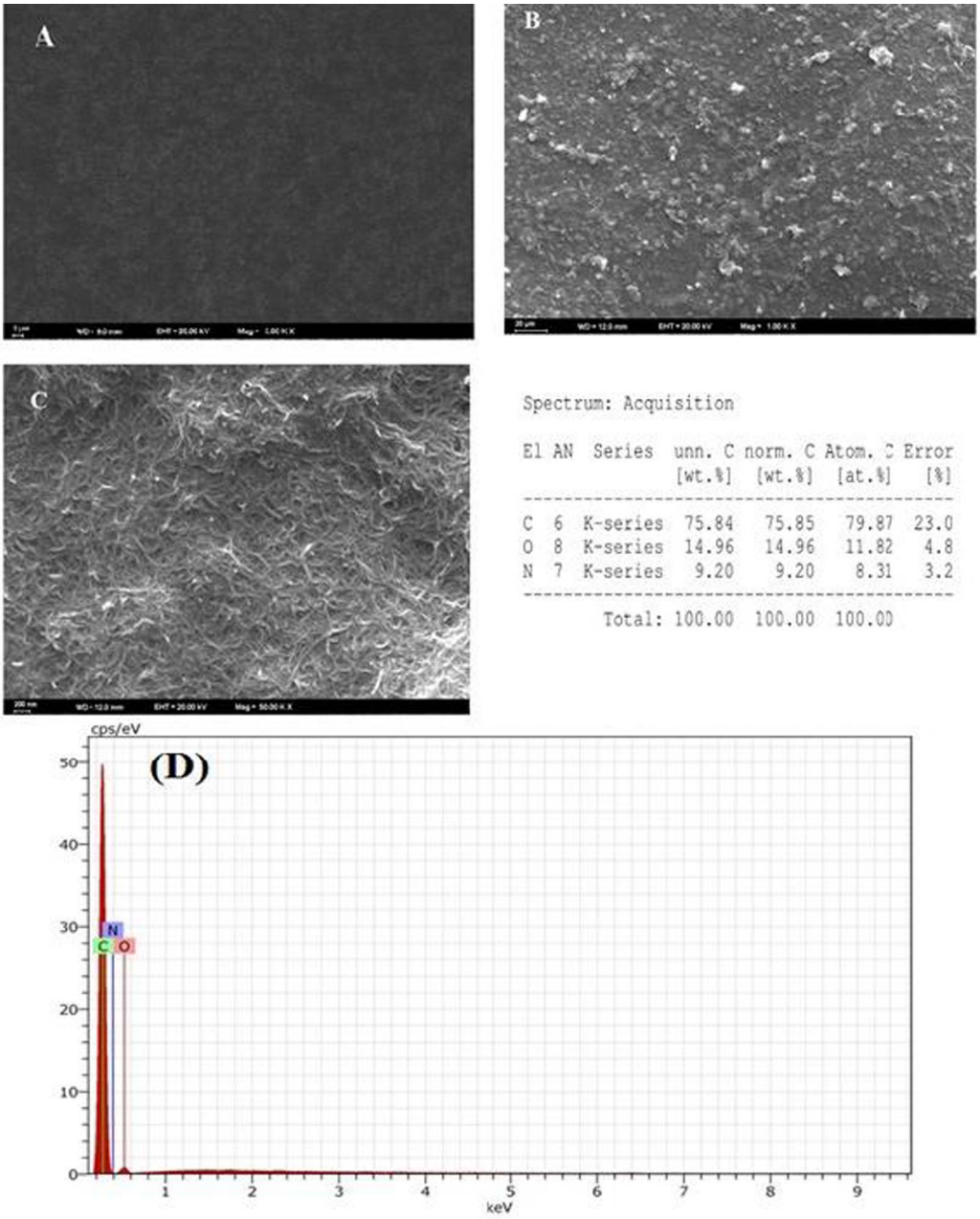


Figure 1. SEM images of (A) bare GCE (at 5μm scale bar); (B-C) NH_2fMWCNTs/GCE (at 10 μm and 100 μm scale bars, respectively); (D) EDX spectra of NH_2fMWCNTs/GCE.

best answer and peak shape of PhA were observed with NH_2*f*MWCNT. NH_2*f*MWCNT showed an electrocatalytic effect, decreasing the peak potential of PhA by 26 mV. It may increase GCE surface area more than other materials.

an electrocatalytic effect, decreasing the peak potential of PhA by 26 mv

The effect of pH.—Considering that one of the key characteristics in electrochemical studies is the pH of supporting electrolyte, the effect of pH was investigated on the oxidation of PhA by DPV at NH_2*f*MWCNT in the range of 2–8. MWCNT can be degraded in more acidic and basic mediums, so that this pH range was studied. The results of the experiments showed that the maximum currents with appropriate peak separation were obtained in pH 3.0 PB solution (Fig. 4A). Acetate buffer solutions (pH: 3.5; 4.5; 5.5) were also studied as well as phosphate buffers. Peak response of PhA was not so sensitive in acetate media. Therefore, PB solution at pH 3.0 was chosen as a supporting electrolyte for subsequent experiments. The influence of pH on peak potential and current was plotted in Figs. 4B and 4C. The oxidation peak potential shifted toward less positive with increasing pH values. The pKa of the amine in PhA is 5.8. It is positively charged at working buffer solution (pH = 3.0).

The E_p versus pH schemes illustrate straight lines with the equations below for first peak and second peak:

$$E_{PI}\,(V) = 1.4444 - 0.0779pH;\ r = 0.99\ (pH\ 2-8) \quad [2]$$

$$E_{P2}\,(V) = 1.1914 - 0.0582pH;\ r = 0.99\ (pH\ 2-8) \quad [3]$$

The −58.2 and −77.9 mV per pH unit shows that equal numbers proton and electron are found in electrochemical oxidation PhA.[32]

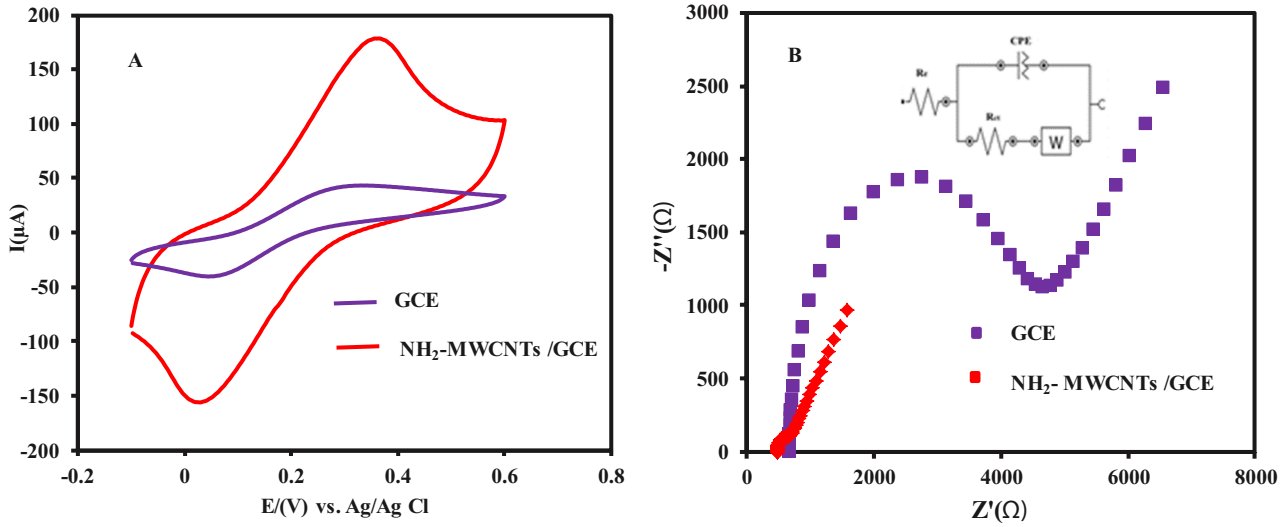


Figure 2. (A) CVs and (B) Nyquist diagram (Z″ versus Z′) for the EIS measurements of GCE (purple line) NH_2fMWCNTs/GCE (red line) in 5 mM $K_3Fe(CN)_6/K_4Fe(CN)_6$.

The effect of potential sweep rate.—In order to evaluate the effect of scan rate on the peak potential and current, CV technique was used. CV was applied at different potential sweep rates between 10 and 500 mVs^{-1} in the presence of 0.1 mM PhA at pH 3.0 PB solution on NH_2*f*MWCNTs/GCE. The results showed that the both anodic peaks of PhA oxidation are linearly proportional to the scan rate, according to following equations:

$$I_{Pl}\ (\mu A) = 0.4472\ v\ (mV s^{-1}) + 4.299;\ r = 0.985 \quad [4]$$

$$I_{P2}\ (\mu A) = 0.2523\ v\ (mV s^{-1}) + 3.0699;\ r = 0.984 \quad [5]$$

$$log\ I_{Pl}\ (\mu A) = 1.1907\ logv\ (mV s^{-1}) - 0.7139;\ r = 0.970 \quad [6]$$

$$log\ I_{P2}\ (\mu A) = 1.1554\ logv\ (mV s^{-1}) - 0.8938;\ r = 0.970 \quad [7]$$

In addition, the relation between logarithm of peak currents of PhA and logarithm scan rate values showed a linearity with slopes of 1.19 and 1.16, for first and second peaks, respectively. These results indicate the adsorption controlled process.

$$\Delta E_p = E_p - E_p/2$$

$$\Delta E_p = \frac{47.7}{\alpha n} mV\ (for\ irreversible\ process\ at\ 25^{\circ}C)^{33,34} \quad [8]$$

According to above equation, 'α' is an electron transfer coefficient and 'n' is the electron number. 'n' is obtained from the difference of peak potential (E_p) and half wave potential ($E_{p/2}$). If α was assumed equal to 0.50, n are equaled 2.38 for first peak and 2.12 for second peak at NH_2*f*MWCNT/GCE that closed to 2 in pH 3.0 PB solution.

Possible oxidation mechanism for PhA.—To investigate the mechanism of electrooxidation PhA, some compounds were studied such as nicotinamide and piroxicam. The model pharmaceutical compounds for PhA mechanism were studied in pH 3.0 PB solution by CV at scan rate 0.1 mV/s (Fig. 5). Nicotinamide did not give similar behavior as PhA due to unelectroactive structure under the studied

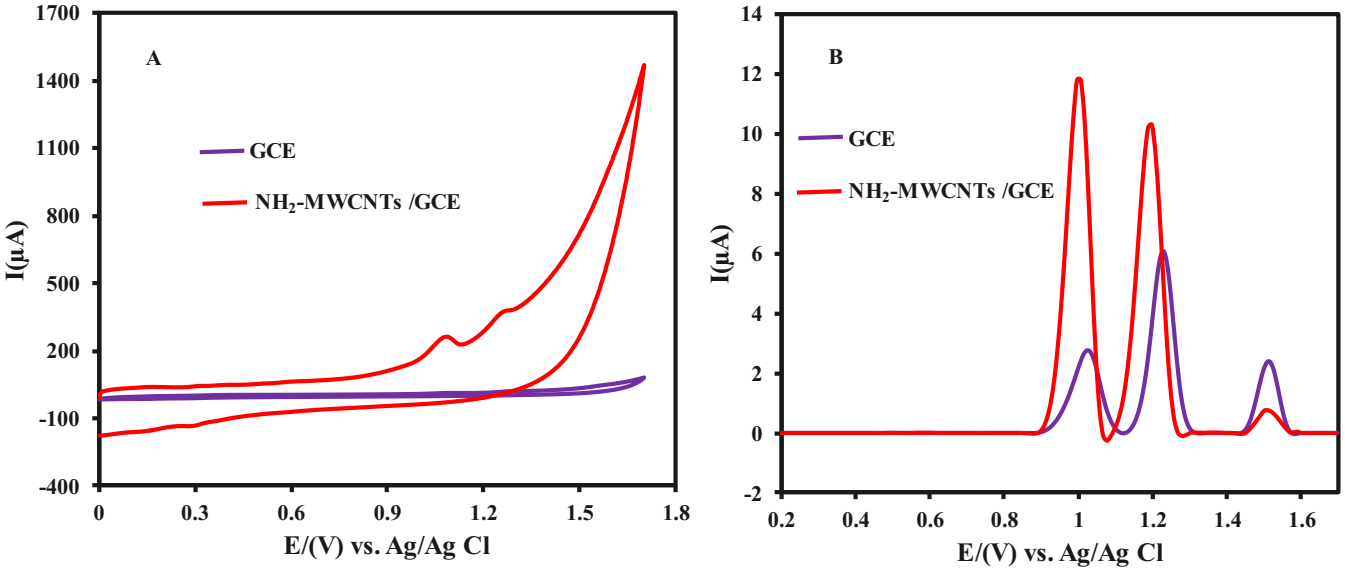


Figure 3. (A) Cyclic voltammograms (CVs) and (B) differential pulse voltammograms (DPVs) of 0.1mM PhA at GCE (purple line) and NH_2fMWCNTs/GCE (red line) in phosphate buffer solution pH 3.0.

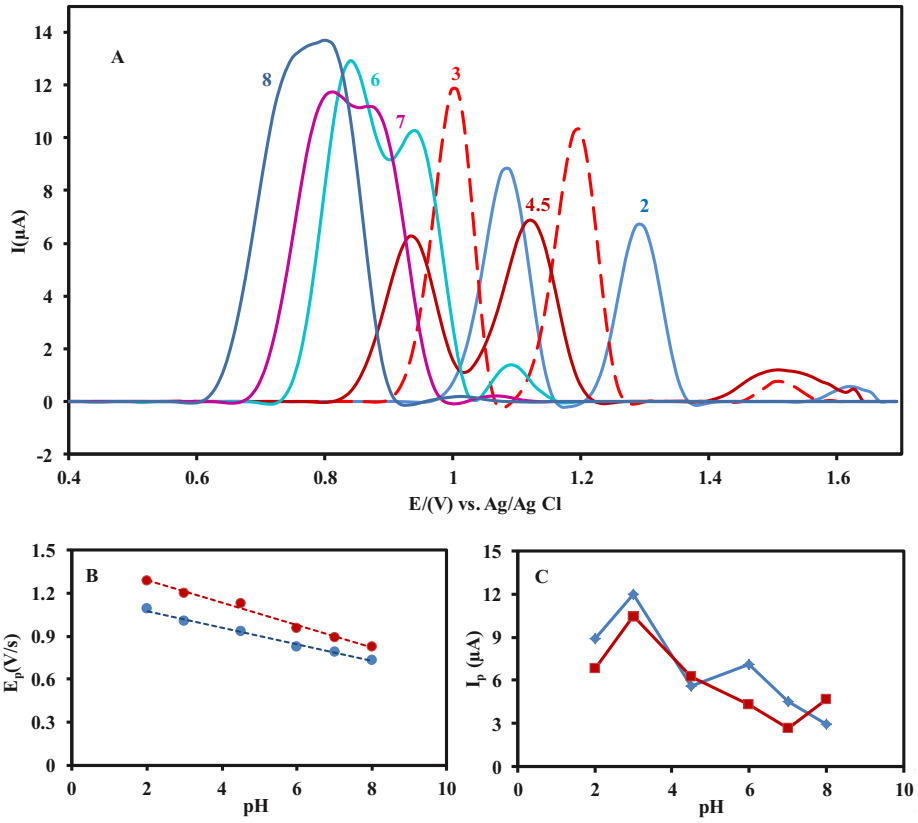


Figure 4. (A) The differential pulse voltammograms, (B) Plots of peak potential and (C) peak current of 0.1mM PhA in different pH (2.0, 3.0, 4.5, 6.0, 7.0, 8.0) at NH_2fMWCNTs /GCE.

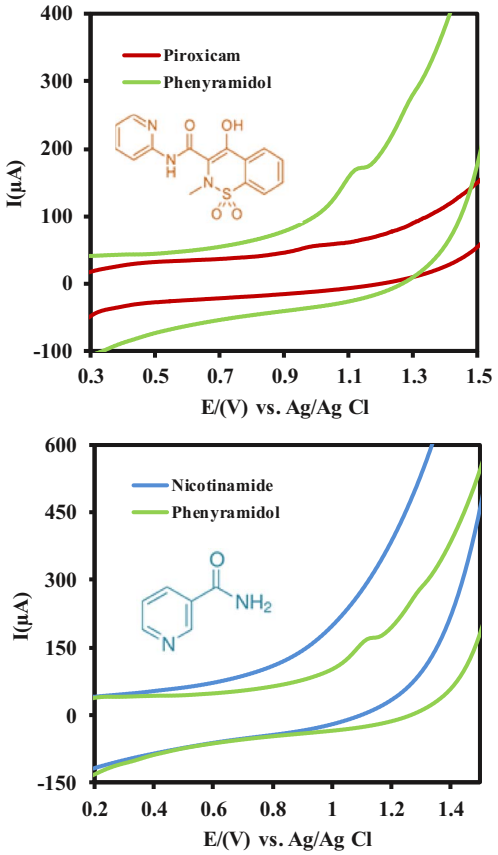


Figure 5. Chemical structures and cyclic voltammograms of 1×10^{-4} M PhA (green line), piroxicam (red line), nicotanamide (blue) at NH_2fMWCNTs/GCE PB solution pH 3.0.

conditions. Piroxicam gave similar response with PhA because of electroactive secondary aniline group.

Aniline oxidation and polyaniline form are well known mechanism in acidic media.[35] Polyaniline can show different oxidation forms due to its degree of oxidation such as emeraldine and pernigraline forms.[35] The possible oxidation mechanism of PhA can be proposed following pathway (Scheme 2):

The effect of accumulation potential and time.—In order to obtain optimized conditions for electrochemical oxidation of 0.1 mM PhA, accumulation time and accumulation potential parameters were studied by AdSDPV using NH_2*f*MWCNTs/GCE. Initially, the effect of accumulation potential (E_{acc}) on the two peak currents of PhA were investigated between potentials of −0.3 to 0 V at 30 s, the potential −0.2 V was selected as the optimal potential, and then the effect of accumulation time (t_{acc}) was studied between 15 and 60 seconds, the best answer was found at 30 s. Hence, further experiments were applied with using −0.2 V and 30 s optimized conditions in PB solution (pH 3.0) (Fig. 6).

DPV and AdSDPV results were compared with 0.1 mM PhA in PB solution (pH 3.0). The oxidation peak currents (I_{P1}, I_{P2}) of PhA increased from 12.01 to 20.9 μA (I_{P1}) and 10.44 to 16.3 μA (I_{P2}) with AdSDPV. The third peak (≈1.5 V) of PhA was also increased with applying stripping (Fig. 7).

Analytical measurement.—*Voltammetric determination.*—For quantitative evaluation of PhA, AdSDPV technique was used under the optimum conditions (Fig. 8). Linearity was observed between 0.8–100 μM for for peak 1 by Eq. 9 and peak 2 by Eq. 10 of PhA.

Using equations of LOD = 3 s/m and the resulted calibration curves, LOD of 6.13×10^{-8} M and 2.78×10^{-8} M were calculated from peaks 1 and 2, respectively.[36]

$$I_{p1}\,(\mu A) = 0.2067\,C\,(\mu M) - 0.0736;\ r = 0.998 \qquad [9]$$

$$I_{p2}\,(\mu A) = 0.1723\,C\,(\mu M) - 0.4782;\ r = 0.998 \qquad [10]$$

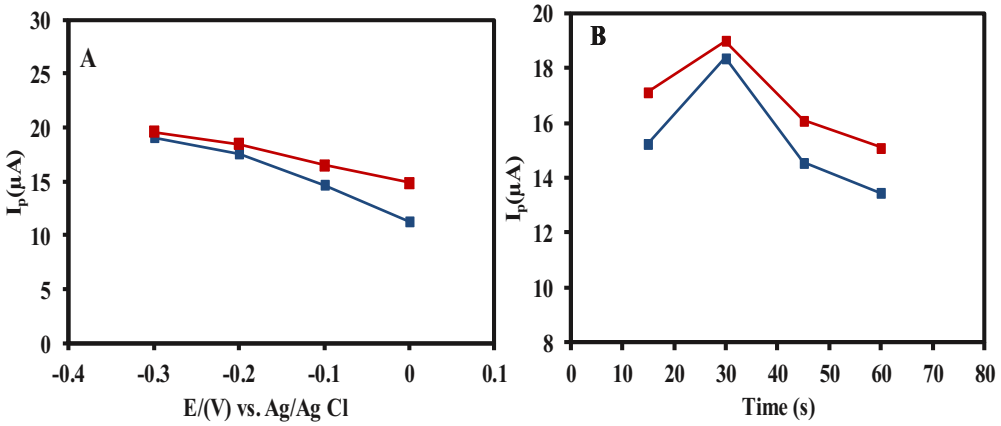


Figure 6. Effect of accumulation potential (A) and accumulation time (B) on peak currents of NH2fMWCNTs/GCE in phosphate buffer solution (pH 3.0) containing 0.1mM PhA.

So far, no method has been proposed for the assay performance characteristics for PhA determination. Therefore, the presented electroanalytical methodology is the proposed at the first time with low detection limit and wide linear dynamic range of PhA (Table I).

Determination of PhA in human serum samples.—For illustrate the practical applications of this method, a calibration graph was drawn using the synthetic human serum. For this purpose, 1×10^{-3} M PhA stock solution in serum was prepared. The linearity range between 1 and 100 μM and the linearity (Figure 9) was acquired with the Equations 11 and 12 for the first and second peaks, respectively.

$$I_{p1}\,(\mu A) = 0.098\,C\,(\mu M) + 0.272;\ r = 0.992 \quad [11]$$

$$I_{p2}\,(\mu A) = 0.081\,C\,(\mu M) - 0.0384;\ r = 0.995 \quad [12]$$

Recovery studies were carried for showing the direct determination of PhA in tablet dosage and spiked human serum by AdSDPV technique without any interferences from excipients and endogenous substances. The results are shown in Table II.

Reproducibility studies and shelf time of developed sensor.—The reproducibility of the nanosensor in the same day and between the days were calculated and their relative standard deviation (RSD %) values are listed in Table I. As shown in Tables I, RSD% obtained for both peaks in the standard solution and serum less than 2% which confirm reproducibility of the proposed method. The shelf-time of proposed electrode on both anodic peaks of PhA oxidation were tested by DPV method under optimum conditions. It was observed that the GCE modified with NH_2*f*MWCNT has one-week shelf-time at least.

The effect of some interference.—The effect of interfering species is one of the most important issues in the analysis of real samples for

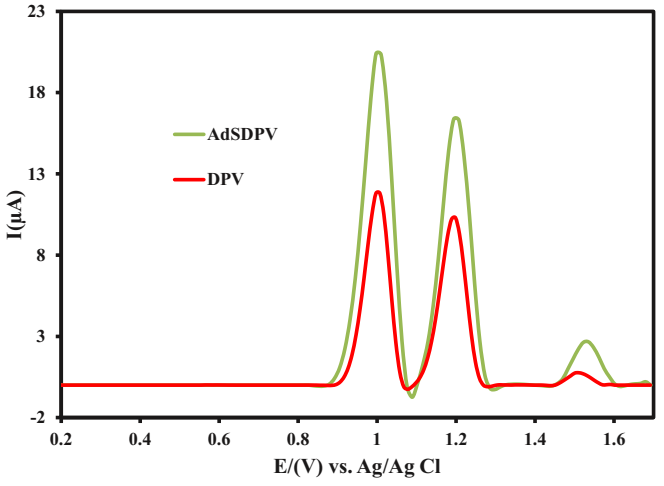


Figure 7. DP (red line) and AdSDP(green line) voltammograms of NH_2fMWCNTs/GCE in phosphate buffer solution (pH 3.0) containing 0.1mM PhA.

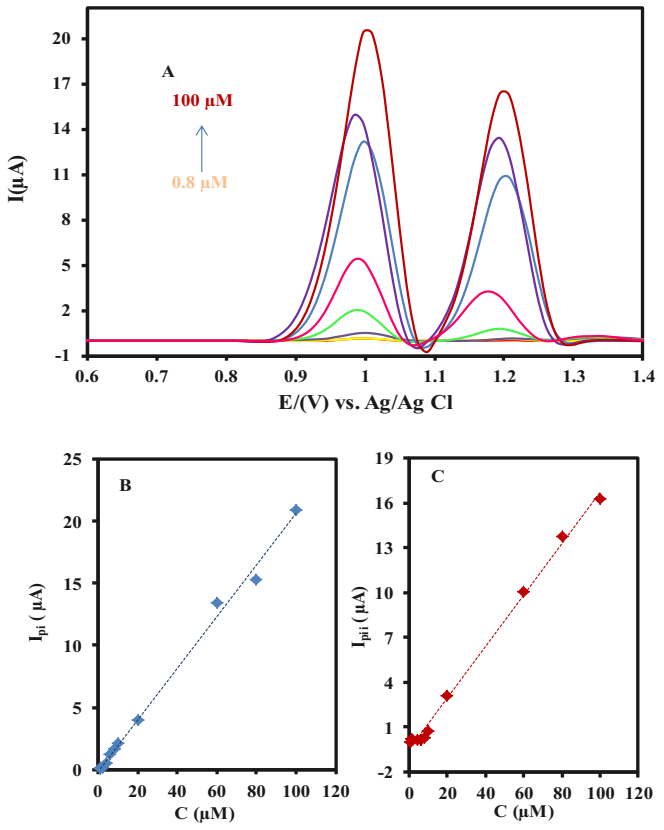


Figure 8. (A) Adsorptive stripping differential pulse voltammograms (AdSDPVs) in various concentrations of PhA at the surface of modified electrode in PB solution pH 3.0, (B-C) Calibration curve: dependency between concentration of PhA with first peak (B) current and second peak (C) current.

Table I. Regression data of the calibration line for quantitative determination of PhA.

	Standard solution		Human serum	
	$Peak_1$	$Peak_2$	$Peak_1$	$Peak_2$
Measured Potential (V)	0.99	1.21	0.99	1.20
Linearity Range (M)	$8 \times 10^{-7} - 1 \times 10^{-4}$	$8 \times 10^{-7} - 1 \times 10^{-4}$	$1 \times 10^{-6} - 1 \times 10^{-4}$	$1 \times 10^{-6} - 1 \times 10^{-4}$
Slope (μAM^{-1})	0.2067	0.1723	0.098	0.081
Intercept (μA)	0.07	0.47	0.272	0.038
Correlation coefficient	0.998	0.998	0.992	0.995
SE of slope	4.83×10^{-3}	3.85×10^{-3}	4.34×10^{-3}	2.72×10^{-3}
SE of intercept	2.09×10^{-7}	1.66×10^{-7}	1.95×10^{-1}	1.28×10^{-1}
LOD (M)	6.13×10^{-8}	2.78×10^{-8}	1.29×10^{-7}	1.77×10^{-7}
LOQ (M)	1.86×10^{-7}	8.44×10^{-8}	3.92×10^{-7}	5.38×10^{-7}
With-in days of peak current (RSD %)*	1.21	1.66	1.61	1.29
With-in days of peak potential (RSD %)*	0.88	0.90	1.53	0.45
Between days of peak current (RSD %)*	1.98	1.77	1.74	1.33
Between days of peak potential (RSD %)*	2.045	1.21	1.67	2.09

*Obtained from five measurements.

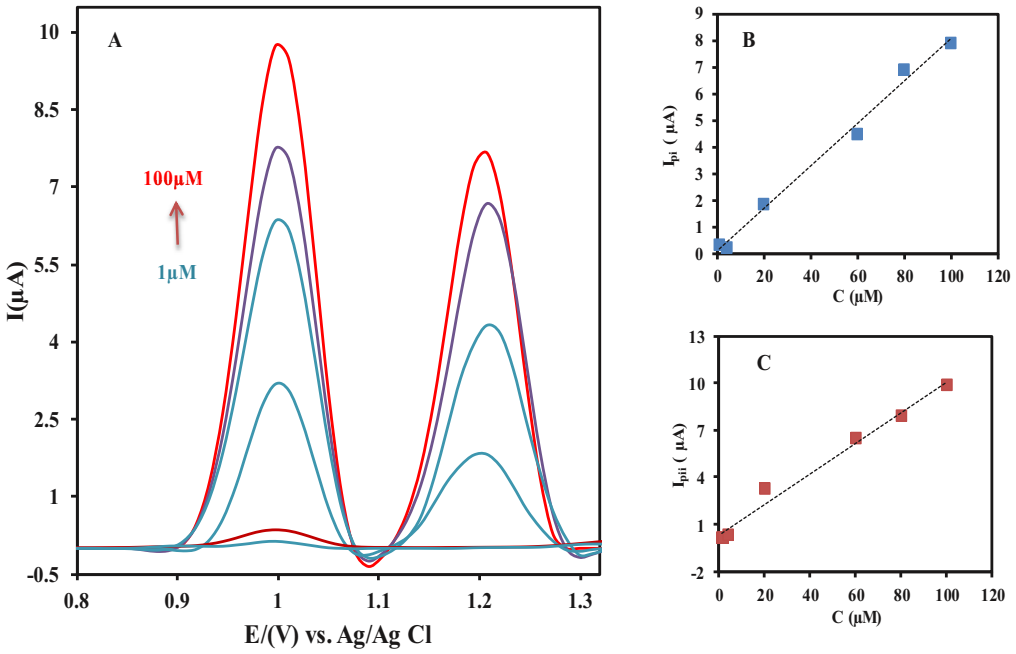


Figure 9. (A) Adsorptive stripping differential pulse voltammograms (AdSDPVs) in various concentrations of PhA at the surface of modified electrode at presence of human serum sample (pH 3.0), (B-C) Calibration curve: dependency between concentration of PhA in the human serum with first peak current (B) and second peak (C) current.

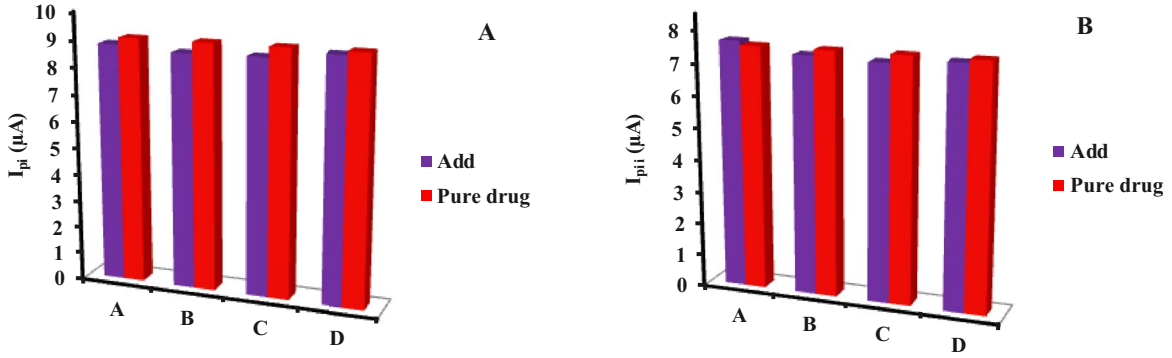


Figure 10. (A-B) bar graphs peak currents of 5×10^{-5} M PhA at PB solution pH 3.0 with NH_2fMWCNTs /GCE in presence of interfering agents(1:1); ascorbic acid+PhA (A), uric acid+PhA (B), sodium chloride+PhA (C) and sodium nitrate+PhA (D) in optimal conditions.

Table II. The results for the determination of PhA from tablet dosage form and synthetic human serum.

	AdSDPV Tablet	AdSDPV Human serum
Labeled claim (mg)	400.00	-
Amount found (mg)[a]	398.55	-
RSD %	1.50	-
Bias %	0.36	-
Added (mg)	200.00	200.00
Found (mg)[a]	200.90	197.32
Average recovered (%)	100.45	98.66
RSD % of recovery	1.22	2.1
Bias %	−0.45	1.34

[a]Obtained from five measurements.

practical applications. Hence, the effects of different interfering substances such as uric acid, ascorbic acid, sodium nitrate and sodium chloride on the PhA (5×10^{-5} M) anodic peak currents were evaluated in pH 3.0 PB solution. From the results, it was found that these compounds have no important effect (less than 5%) on PhA signals (Fig. 10).

Conclusions

PhA is an analgesic and relaxant drug which is common used for medicinal treatment of chronic muscular disorders. Electrochemical methods are so popular by researchers due to their sensitive analysis of pharmaceuticals, biomolecules, viruses and bacteria. The present research illustrates an approach for the development of a voltammetric phenyramidol HCl sensor for the first time. The working electrode is modified with NH_2*f*MWCNT for creating a nanosensor. This nanosensor has demonstrated high electrocatalytic activity toward PhA oxidation in pH 3.00 phosphate buffer solution. The effect of modifier type, pH influence, scan rate, accumulation potential and time were studied as details to get the best response for the determination of PhA. The results showed that GCE modified with NH_2*f*MWCNT is an effective nanosensor with easy preparation and high sensitivity for electro-oxidation of PhA with LOD value of 6.13×10^{-8} M and 2.78×10^{-8} M for peaks 1 and 2, respectively. NH_2*f*MWCNT/GCE was performed for the determination of phenyramidol HCl in commercial tablet and human serum, successfully. The proposed nanosensor in this work revealed to relatively fast response, high selectivity and sensitivity. In future, this sensor may be applied for fast detection of PhA in patient serum sample as on-site application. The diagnosis and treatment of diseases are very crucial for patients and health professionals. This type of studies can be important for developing lab on a chip technology in clinical studies.

Acknowledgments

The authors are grateful to the Ministry of Science, Research and Technology of Iran for financial support.

ORCID

Sibel A Ozkan https://orcid.org/0000-0001-5469-9142

References

1. T. B. O'Dell, L. R. Wilson, M. D. Napoli, H. D. White, and J. H. Mirsky, *J. Pharmacol. Exp. Ther.*, **128**, 65 (1960).
2. Y. Orak, T. Barçın, and F. Orak, *Türk Yoğun Bakım Derneği Dergisi*, **11**, 80 (2013).
3. H. Shah, A. Shakeel, N. Karne, C. Patil, R. Kewalramani, V. Kasodekar, and M. Dave, *Open Access Journal of Clinical Trials*, **3**, 27 (2011).
4. H. Ergün, O. Polat, N. A. Demirkan, M. Günalp, and S. Gürler, *Turk J Med Sci*., **40**, 71 (2010).
5. M. Govindasamy, S. Manavalan, S.-M. Chen, U. Rajaji, T.-W. Chen, F. M. Al-Hemaid, M. A. Ali, and M. S. Elshikh, *J. Electrochem. Soc.*, **165**, B370 (2018).
6. S. Yang, M. Yang, Q. Liu, X. Wang, H. Fa, Y. Wang, and C. Hou, *J. Electrochem. Soc.*, **166**, B547 (2019).
7. G. Karim-Nezhad, Z. Khorablou, and P. S. Dorraji, *J. Electrochem. Soc.*, **163**, B358 (2016).
8. L. Fotouhi, P. S. Dorraji, Y. S. S. Keshmiri, and M. Hamtak, *J. Electrochem. Soc.*, **165**, B202 (2018).
9. R. Lin, T. M. Lim, and T. Tran, *Electrochem. Commun.*, **86**, 135 (2018).
10. S. Iijima, *nature*, **354**, 56 (1991).
11. W. Yang, P. Thordarson, J. J. Gooding, S. P. Ringer, and F. Braet, *Nanotechnology*, **18**, 412001 (2007).
12. G. Hong, S. Diao, A. L. Antaris, and H. Dai, *Chem. Rev*, **115**, 10816 (2015).
13. Z. Liu, M. Jin, J. Cao, J. Wang, X. Wang, G. Zhou, A van den Berg, and L. Shui, *Sensors and Act. B: Chemical*, **257**, 1065 (2018).
14. R. H. Baughman, A. A. Zakhidov, and W. A. De Heer, *science*, **297**, 787 (2002).
15. C. Yang, M. E. Denno, P. Pyakurel, and B. J. Venton, *Chim. Acta.*, **887**, 17 (2015).
16. J. Wang, *Electroanalysis: Electroynalysis (N.Y.N.Y.)*, **17**, 7 (2005).
17. S. Kurbanoglu, M. A. Unal, and S. A. Ozkan, *Electrochim Act*., (2018).
18. G. Ozcelikay, S. Kurbanoglu, B. Bozal-Palabiyik, B. Uslu, and S. A. Ozkan, *J. Electroanal Chem.*, **827**, 51 (2018).
19. S. Aftab, G. Ozcelikay, S. Kurbanoglu, A. Shah, F. J. Iftikhar, and S. A. Ozkan, *J. Pharm Biomed Anal.*, (2018).
20. X. Wang, L. Yang, X. Jin, and L. Zhang, *Food Chem*., **157**, 464 (2014).
21. T. A. Freitas, A. B. Mattos, B. V. Silva, and R. F. Dutra, *BioMed Res. Int.*, 2014 (2014).
22. N. A. Abdallah and S. Ahmed, *J. Electrochem. Soc.*, **165**, H756 (2018).
23. A. S. Ahammad, T. Akter, A. Al Mamun, T. Islam, M. M. Hasan, M. Mamun, S. Faraezi, F. Monira, and J. K. Saha, *J. Electrochem. Soc.*, **165**, B390 (2018).
24. T. Zhao, L. Liu, G. Li, A. Dang, and T. Li, *J. Electrochem. Soc.*, **159**, K141 (2012).
25. Y. Sang, B. Wang, Q. Wang, G. Zhao, and P. Guo, *Sci. Rep.*, **4**, 6321 (2014).
26. Y. Sang, A. Fu, H. Li, J. Zhang, Z. Li, H. Li, X. Zhao, and P. Guo, *Colloids Surf. A.*, **506**, 476 (2016).
27. H. Bi, Y. Li, S. Liu, P. Guo, Z. Wei, C. Lv, J. Zhang, and X. Zhao, *Sens Actuators B Chem*., **171**, 1132 (2012).
28. S. Aftab, S. Kurbanoglu, G. Ozcelikay, N. K. Bakirhan, A. Shah, and S. A. Ozkan, *Sens Actuators B Chem*., **285**, 571 (2019).
29. J. Huang, Y. Liu, H. Hou, and T. You, *Biosens. Bioelectron.*, **24**, 632 (2008).
30. B. J. Matsoso, B. K. Mutuma, C. Billing, K. Ranganathan, T. Lerotholi, G. Jones, and N. J. Coville, *J. Electroanal. Chem.*, **833**, 160 (2019).
31. R. Sha, N. Vishnu, and S. Badhulika, *S Sens Actuators B Chem*., **279**, 53 (2019).
32. R. N. Goyal, N. Bachheti, A. Tyagi, and A. K. Pandey, *Anal. Chim. Acta.*, **605**, 34 (2007).
33. D. Pletcher, R. Greff, R. Peat, Peter, and J. Robinson, *Instrumental methods in electrochemistry*, Elsevier (2001).
34. H. Imanzadeh, N. K. Bakirhan, B. Habibi, and S. A. Ozkan, *J. Electrochem. Soc.*, **166**, B933 (2019).
35. M. Mitadera, N. Spataru, and A. Fujishima, *J. Appl. Electrochem.*, **34**, 249 (2004).
36. S. Ozkan, J.-M. Kauffmann, P. Zuman, A. M. Oliveira Brett, C. Brett, B. Uslu, P. Hubert, E. Rozet, C. Parsajoo, and S. Patris, Electroanalysis in Biomedical and Pharmaceutical Sciences: Voltammetry, Amperometry, Biosensors, Applications, *Springer-Verlag Berlin Heidelberg*, **1**, 350 (2015).